fibers

MDPI

Article

Effect of Cenosphere Fillers on Mechanical Strength and Abrasive Wear Resistance of Carbon–Glass Polyester Composites

K. H. Pulikeshi [1,2,*], Dayanand M. Goudar [3], R. V. Kurahatti [1] and Deesy G. Pinto [4,5,*]

[1] Department of Mechanical Engineering, Basaveshwar Engineering College, Bagalkote 587101, India
[2] Department of Mechanical Engineering, Visvesvaraya Technological University, Belagavi 590018, India
[3] Department of Mechanical Engineering, Tontadaraya College of Engineering, Gadag 582101, India; dmgoudartce@gmail.com
[4] GeoBioTec, Department of Civil Engineering and Architecture, University of Beira Interior, Calçada Fonte do Lameiro 6, 6200-358 Covilhã, Portugal
[5] Department of Civil Engineering & Geology, University of Madeira, Campus da Penteada, 9020-105 Funchal, Portugal
* Correspondence: pulikeshi86@gmail.com (K.H.P.); deesy.gp.correia@ubi.pt or deesy.pinto@staff.uma.pt (D.G.P.)

Highlights

What are the main findings?

- Cenosphere-filled carbon–glass fabric-reinforced polyester composites exhibit a 30–50% reduction in wear rate compared to unfilled composites;
- The addition of cenospheres improves the mechanical properties of the composites, with a 20–30% increase in tensile strength and stiffness.

What is the implication of the main finding?

- The optimal use of cenospheres as fillers in hybrid polymer composites can enhance their tribological and mechanical performance, leading to improved durability and lifespan in industrial applications.
- The development of cenosphere-filled carbon–glass fabric-reinforced polyester composites can address the growing demand for advanced materials in industries such as aerospace, automotive, and construction.

Abstract: Fabric-reinforced hybrid polymer composites are present in almost every sector of modern life, and most essential areas of research in recent years have focused on glass–carbon fabric with filler material composites. Fabric and fillers are employed in strengthening polymer composites with the aim of improving their mechanical and tribological properties. The primary objective of this investigation was to investigate thetribological and mechanical properties of unfilled and cenosphere-filled carbon–glass-reinforced polyester composite systems, utilizing two types of fabric (glass and carbon) with cenosphere filler in varying weight fractions (0, 2.5, 5, 7.5, 10, and 12.5 wt.%) for both carbon fabric and the cenosphere. The abrasive wear characteristics were evaluated using a stainlesssteel wheel abrasion tester, utilizing silica sand as the abrasive material. Tests were performed at various distances (360–1800 m) and loads (12 N and 24 N). The results show that the wear rate of carbon–glass fabric-reinforced polyester composites differs significantly, with and without cenosphere fillers. Notably, the unfilled composites exhibit the highest wear volume loss, indicating a substantial improvement in wear resistance with the addition of cenospheres. The results reveal that in carbon–glass fabric-reinforced polyester composites, specific wear rate decreases when more cenospheres are loaded. The wear rate was successfully reduced by cenospheresunder silica sand as an abrasive. Compared to unfilled composites, the

Academic Editor: Catalin R. Picu

Received: 28 December 2024
Revised: 6 March 2025
Accepted: 3 April 2025
Published: 14 April 2025

Citation: Pulikeshi, K.H.; Goudar, D.M.; Kurahatti, R.V.; Pinto, D.G. Effect of Cenosphere Fillers on Mechanical Strength and Abrasive Wear Resistance of Carbon–Glass Polyester Composites. *Fibers* **2025**, *13*, 46. https://doi.org/10.3390/fib13040046

mechanical properties of filled composites exhibit superior performance. These variations were explained by examining the worn-out surfaces under an SEM and correlating the features observed with the mechanical properties.

Keywords: carbon fabric; glass fabric; unsaturated polyester; cenosphere; hand layup; abrasive wear

1. Introduction

Polymers matrix composites (PMC) have emerged as a promising material for various wear-critical applications, including seals, bearings, and prosthetics. Their unique combination of high strength, corrosion resistance, and self-lubrication makes them an attractive choice for these applications [1]. Polymer matrix composites (PMCs) have been enhanced through various material processing techniques, incorporating reinforcements like glass, carbon, and aramid fibers, as well as organic and inorganic fillers, to significantly improve their wear performance and overall characteristics. The mechanical and tribological performance of particulate-filled composites is profoundly influenced by the quality of interfacial adhesion between the filler particles and the polymer matrix, as well as the physical and chemical attributes of the filler particles. Substantial research efforts have been directed towards understanding the wear performance of particulate and fiber-reinforced polymer composites [2–8]. The wear process in fiber-reinforced polymer composites is characterized by a multifaceted interaction between the matrix, reinforcement, and coupling agents, resulting in the production of wear debris. The performance of these composites under abrasive wear can be affected by the addition of fibers in both positive and negative ways. The incorporation of fibers as reinforcing materials enhances the mechanical and tribological properties of composites, while also reducing production costs. To further optimize composite performance, extensive research has been conducted on various fillers and fiber-reinforced polymer composites, exploring their potential to improve overall product quality and efficiency. Research has previously emphasized the outstanding wear resistance of fiber-reinforced polymer composites, which can be attributed to their superior elastic stiffness, notable interlaminar shear strength, and inherent self-lubricating characteristics [9]. Carbon fiber is extensively utilized as reinforcement in polymer matrices, owing to its superior mechanical characteristics, such as high tensile strength, modulus, and thermal stability. Studies on the mechanical and abrasive wear behavior of vinyl ester composites reinforced with glass and carbon fibers have shown significant improvements in mechanical properties and reduced wear rates. Additionally, the incorporation of silicon carbide fillers in glass fabric–vinyl ester composites has been found to enhance abrasive wear performance, outperforming graphite-filled composites [10]. The production of cenospheres as a thermal power plant byproduct poses significant recycling challenges. Research is in progress concerning various methods for exploiting this byproduct to cope with environmental challenges and efficiently develop new usable materials. Cenosphere, distinguished by a tremendously low density of less than 0.7 g/cm^3, can be utilized for the fabrication of lightweight polymer matrix composites (PMCs). In the decade since then, Cenospheres have been integrated into a range of matrices, including cement, polyester, and epoxy, to produce composite materials for various industrial applications [11–13]. Studies have demonstrated that the addition of red mud as a filler in epoxy composites enhances their wear resistance. The use of industrial waste materials as fillers in polymer composites has garnered significant research attention, driven by the potential benefits of reduced waste disposal and enhanced material sustainability [14]. The addition of coal combustion-derived fillers to glass-epoxy composites has been investigated, demonstrating

the feasibility of leveraging industrial waste materials to improve the tribological performance of polymer composites [15]. The incorporation of particulate reinforcements has been found to significantly improve the wear behavior of composites [16]. The integration of fly ash cenospheres (FAC) into glass-epoxy (G-E) composites resulted in a substantial reduction in the coefficient of friction and wear rate [17]. Furthermore, research has demonstrated that the addition of micro-fillers can decrease the wear rate of fiber-reinforced epoxy-based micro-composites, particularly under high loads and abrading distances [18]. The incorporation of cenospheres, a type of lightweight and hard ceramic material, as fillers in these composites is hypothesized to enhance their wear resistance. Adding cenospheres lies in their potential to improve the strength-to-weight ratio, toughness, and thermal stability of the composites. Moreover, the hollow structure of cenospheres reduces the density of the material, making it an ideal candidate for lightweight applications. Therefore, investigating the mechanical properties of cenospheres-reinforced composites is crucial to understanding their potential industrial applications. This study aims to explore the effects of cenosphere fillers on the mechanical behavior and abrasive wear resistance of carbon–glass fabric-reinforced polyester composites. Wear tests are conducted under varying loads and sliding speeds to assess the composites' performance. To optimize filler concentration, composites with cenosphere weight fractions ranging from 0 to 12.5 wt.% are systematically evaluated.

2. Materials and Methods

2.1. Materials

The PMC°s are synthesized using bidirectional carbon–glass fabric yarn as reinforcement, with yarn diameters ranging from approximately 6 to 8 mm. For the matrix material, an unsaturated polyester (MEKP) resin and cobalt Napthanate-grade room temperature curing hardener mix all provided by LeoEnterprise (Nagercoil, Tamilnadu, India) were used. Cenospheres, lightweight, inert, hollow spheres primarily comprising silica and alumina, were employed as secondary reinforcement. These spheres, a byproduct of coal combustion at thermal power plants, had a particle size range of 5–70µm (Kulin Corporation, Mumbai, India). The chemical composition and physical properties of cenosphere powder are summarized in Tables 1 and 2, respectively. Photographs of glass fiber fabric, carbon fibers fabric, and cenosphere particles are shown in Figure 1. The laminates, with a thickness of 3.5 mm, were fabricated by stacking eight layers of fabric using the hand lay-up method. A uniform mixture of resin and cenospheres was evenly distributed between the stacked fabric layers. To maintain a consistent thickness, the assembly was placed in a $300 \times 120 \times 3.5$ mm^3 mold. The mold was then subjected to 0.5 MPa pressure in a hydraulic press and cured at an ambient temperature for 24 h. To fabricate the C-G-P laminate, the resin mixture was combined with the requisite quantity of hardener and then supplemented with cenospheres in varying weight fractions to produce both unfilled and filled composite samples. The fabrication process is illustrated in Figure 2, which depicts the hand lay-up technique used to create the hybrid composites. The physical and mechanical properties of S-Glass fiber, carbon fabric, andcenosphere reinforcements are summarized in Table 1 and the chemical composition of the cenosphere is listed in Table 2.

Table 1. Physical and mechanical properties of reinforcements [19].

Sl No	Properties	S-Glass Fiber	Carbon Fabric	Cenosphere
1	Density (g/cm^3)	2.49	1.79	0.37
2	Compressive Strength (MPa)	--	--	23.56
3	Hardness (Mohs)	--	--	5.67
4	Melting Point (°C)	---	--	1350
5	Particle Size (nm)	----	--	5–70
6	Tensile Strength (MPa)	4600	5407	--
7	Elongation (%)	5.5	1.75	-----

Table 2. Cenosphere chemical composition (wt.%) [20].

SiO_2	Al_2O_3	K_2O	Fe_2O_3	TiO_2	MgO	Na_2O	CaO
55.4	31.1	3.2	4.13	1.3	2.3	1.2	1.4

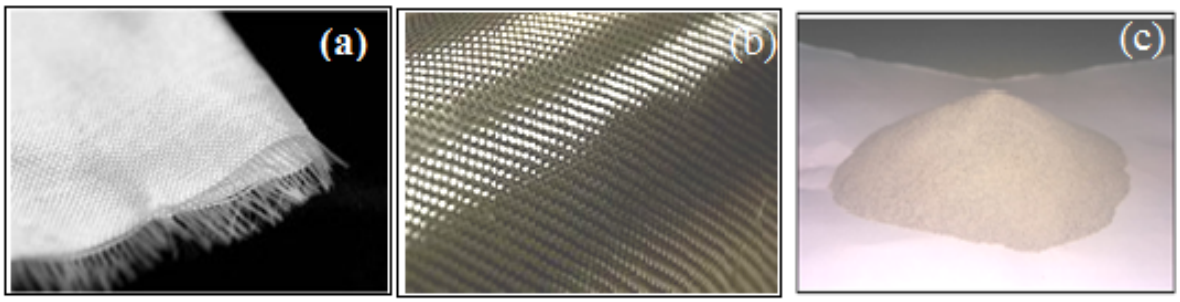

Figure 1. Photographs of (**a**) glass fibers fabrics, (**b**) carbon fiber fabrics, and (**c**) cenosphere particles.

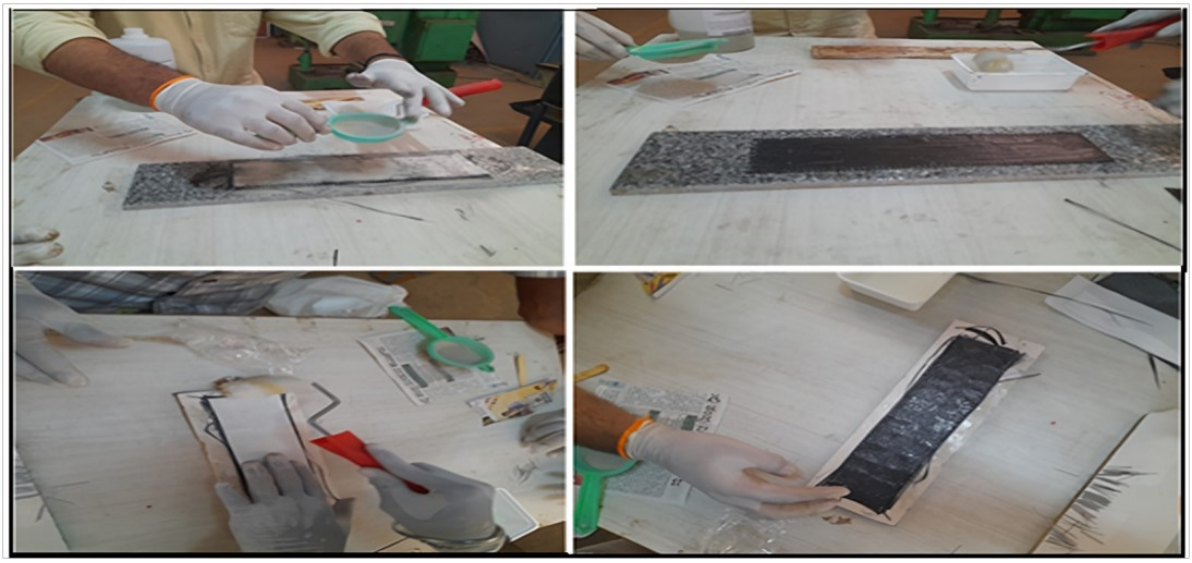

Figure 2. Fabrication of hybrid composites by hand lay-up technique.

The designation of composites and composition of the composites with and without cenosphere filler material are listed in Table 3 and Table 4, respectively.

Table 3. Composition of the composites without filler material.

Composites Sample Code	GF wt.%	CF wt.%	Resin wt.%
C1	0	50	50
C2	50	0	50
C3	50	2.5	47.5
C4	50	5	45
C5	50	7.5	42.5
C6	50	10	40
C7	50	12.5	37.5

CF: Carbon-reinforced composite; GF-Glass-reinforced composite.

Table 4. Composition of the composites with filler material (cenosphere).

Composites Code	GF wt.%	CF wt.%	Polyester Resin wt.%	Cenosphere wt.%
C6-CN-2.5	50	10	37.5	2.5
C6-CN-5	50	10	35	5
C6-N-7.5	50	10	32.5	7.5
C6-CN-10	50	10	30	10
C6-CN-12.5	50	10	27.5	12.5

CN—Cenosphere.

2.2. Mechanical Characterization

2.2.1. Tensile Test

All samples were examined in tensile mode employing the Instron universal testing instrument (Model 1125) adhering to ASTM D638, with a dimension of 165 mm × 13 mm × 3.5 mm (gauge length = 50 mm),and subjected to uniaxial tension at a constant crosshead speed of 2.5 mm/min. Five replicate tests were performed for each sample, and their mean values were calculated and reported. Tensile-fractured specimen C1, C2,C6, and C6-CN-10 composites are shown in Figure 3

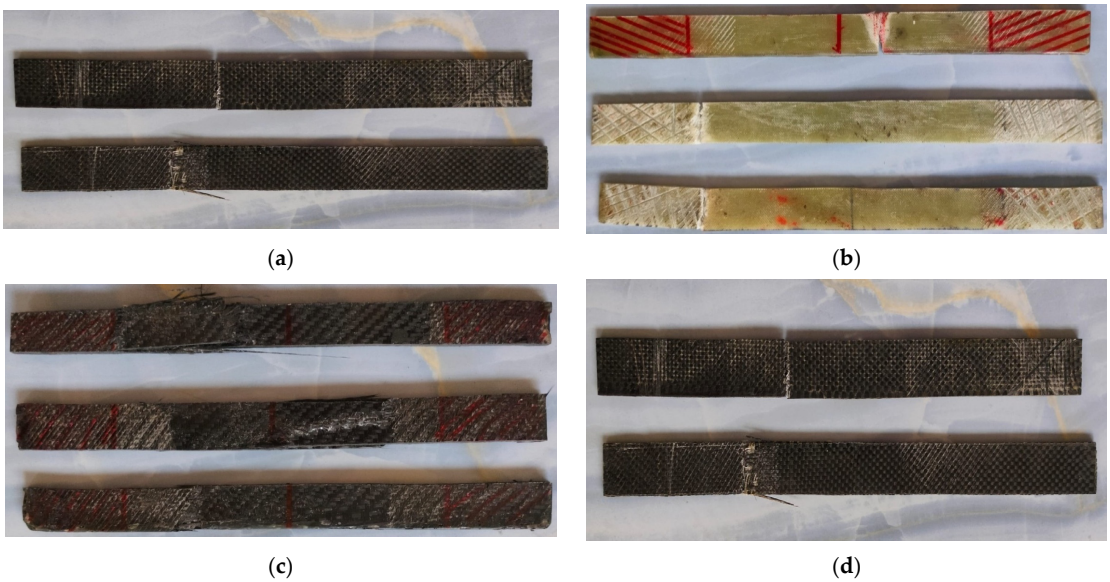

Figure 3. Tensile-fractured specimen (**a**) C1, (**b**) C2, (**c**) C6, and (**d**) C6-CN-10 composites.

2.2.2. Hardness Test

The hardness of the composite materials was assessed using the Shore D hardness test, in accordance with standard test procedures. The test specimen was placed on a firm, flat surface, and the Shore D durometer was positioned on the specimen, ensuring the indenter was perpendicular to the surface. The durometer was pressed down slowly and steadily until the indenter made contact with the specimen and then held in place for 1–2s to allow the indenter to penetrate the surface. The hardness value was then read on the durometer scale, and the test was repeated five times, spaced evenly apart, to ensure consistent results. The average hardness value was recorded and reported, usually expressed in units of Shore D.

2.2.3. Charpy Impact Test

The composite materials' ability to absorb impact was determined using the Charpy impact test, conforming to ASTM D6110-18 standards. Test specimens were prepared as per standard procedure and a notch was made using a diamond-coated saw blade with a precision cutting machine. The notch was carefully crafted to ensure a precise depth and width, with a radius of approximately 0.1–0.2 mm at the notch tip. Specimens measuring 130 mm × 13 mm × 3.5 mm were tested, with five replicates per composition. The impact test was conducted at a drop height of 140 mm, generating an impact force of 196.2 N. Figure 4 shows the photographs of samples of before (a–c) and after (d–f) the impact test.

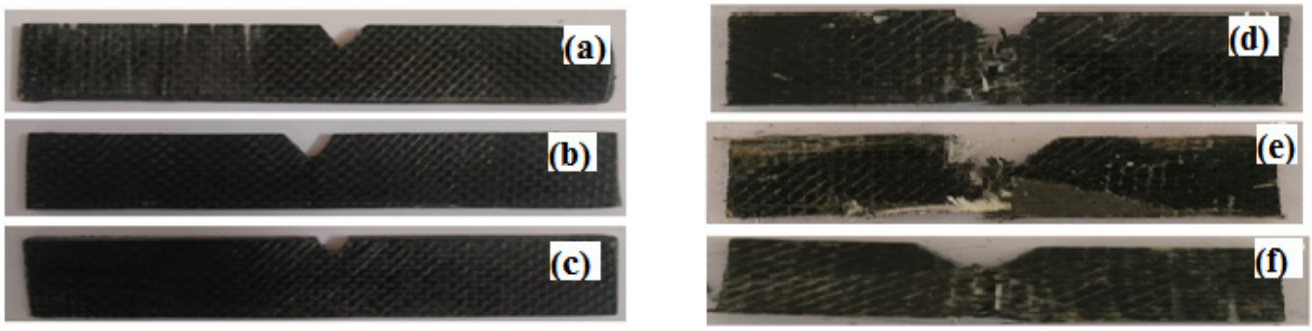

Figure 4. (**a**–**c**) Pre-test sample photographs of C1, C2, and C3 and (**d**–**f**) tested sample photographs of C1, C2, and C3.

2.2.4. Abrasion Test

Abrasive wear characteristics were evaluated using a dry sand/stainless steel wheel abrasion tester, conforming to ASTM G65 protocol. The test setup consisted of a rotating stainless-steel wheel (220 mm diameter) and a controlled flow of silica sand abrasives with a density of 2.6 g/cm^3 and a Knoop hardness of 875. Specimens were prepared by cleaning, drying, and accurate weighing (±0.1 mg). Experiments were performed at 200 RPM, with an abrasive feeding rate of 255 g/min. A lever arm applied a defined force against the rotating wheel, while a regulated flow of abrasives eroded the test surface. After testing, specimens were cleaned, weighed, and the weight loss was calculated. The abrasive wear testing was performed at loads of 12 N and 24 N, with a sliding velocity of 2.15 m/s, and abrading distances ranging from 360 m to 1800 m. Three tests were conducted, with mean values reported. Wear rates were determined from weight loss data and quantified as volume loss.

The specific wear rate (Ks) was determined using the following formula:

$$Ks = \Delta V/(L \times D) \quad (1)$$

where ΔV represents the volume loss, L is the applied load, and D is the abrading distance.

The surface morphology of the worn-out specimens was examined using a scanning electron microscope (JEOL). The SEM analysis was performed under optimal conditions, with an accelerating voltage of 10–20 kV, and the working range was 100 µm.

3. Results and Discussion

3.1. Mechanical Properties

Figure 5 illustrates the mechanical properties of composites, comprising varying carbon fabric content (C2, C3, C4, C5, C6, C7 wt.%) and a 50 wt.% glass fabric (C1). It is observed that significant increases are noticed: tensile strength (σ) increases by 12%, tensile modulus (E) by 19%, impact strength by 13%, and hardness by 19% when assessing composites from 2.5 wt.% to 10 wt%. Table 5 displays the composites' mechanical test results for each of the five samples.

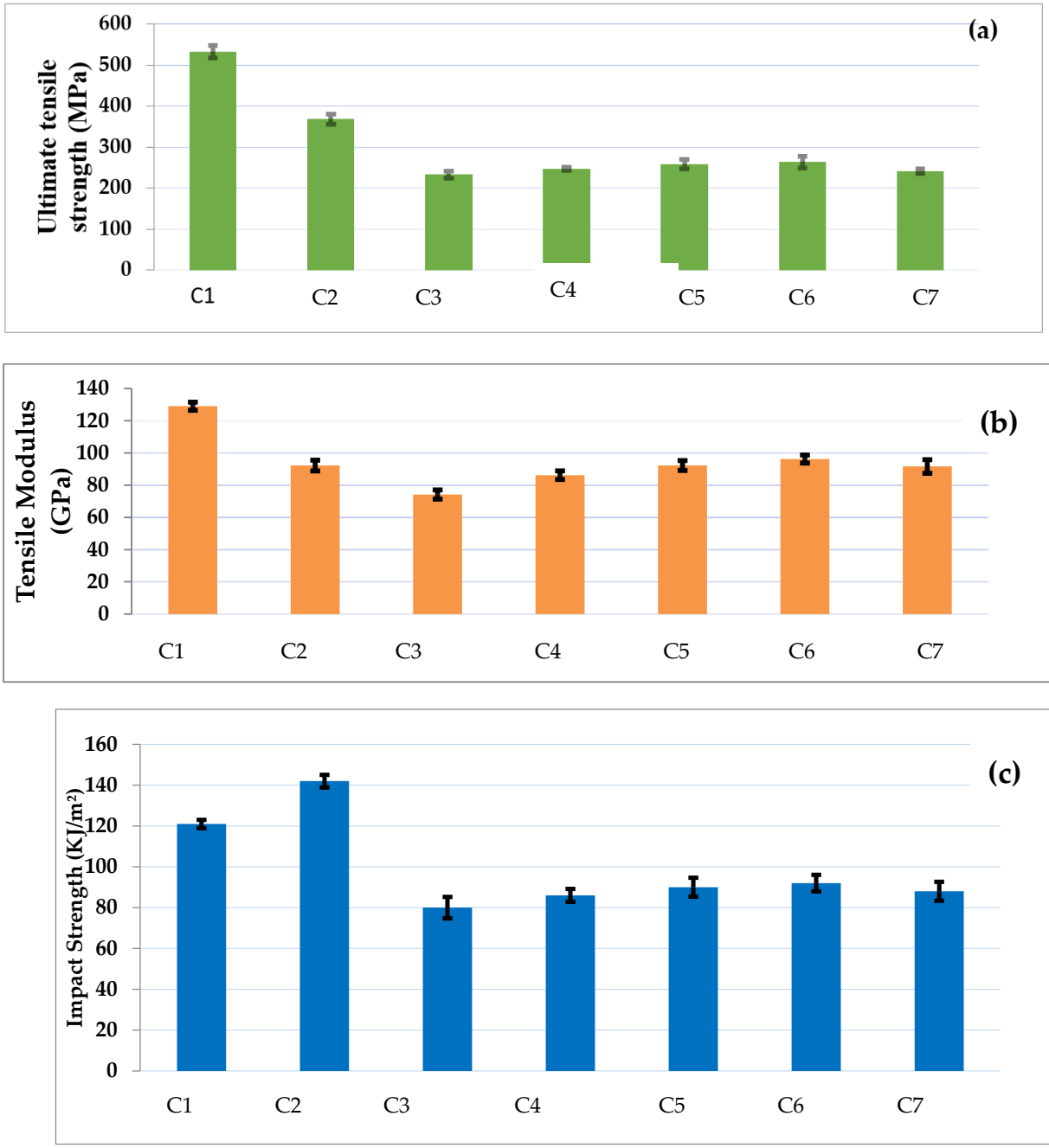

Figure 5. *Cont.*

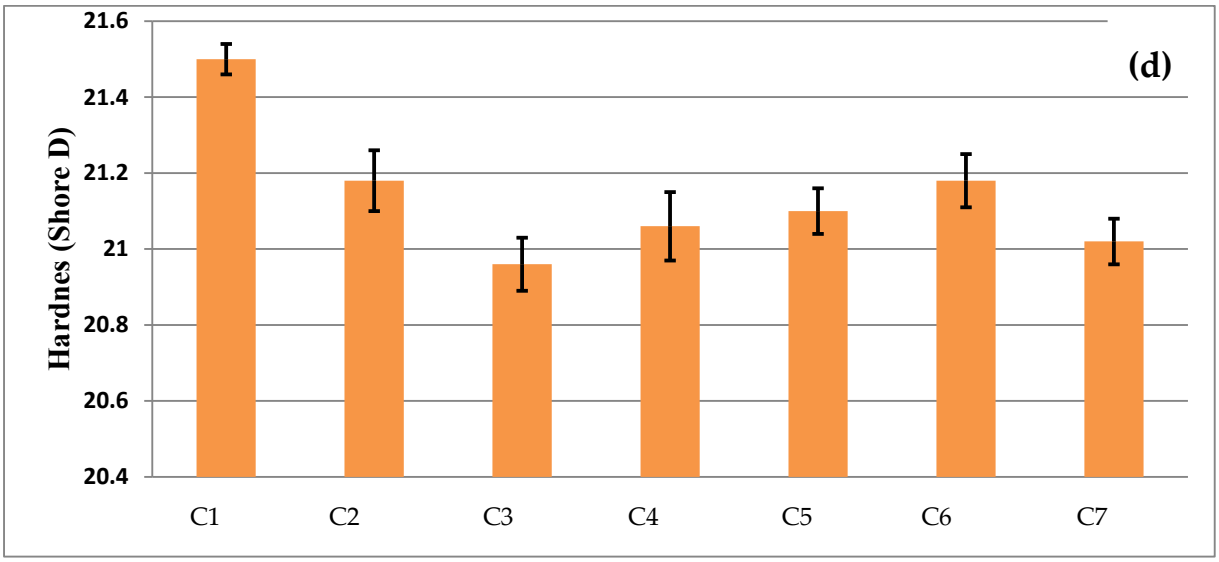

Figure 5. Mechanical properties of composites. (**a**) Tensile strength, (**b**) tensile modulus, (**c**) impact strength, and (**d**) shore D hardness.

Table 5. a. Ultimate tensile strength (MPa). b. Tensile modulus (GPa). c. Hardness (shore D).

a.						
Composite	**Sample 1**	**Sample 2**	**Sample 3**	**Sample 4**	**Sample 5**	**Std. Deviation**
C1	532	560	521	524	526	±15.8
C2	370	382	359	352	378	±12.5
C3	236	241	232	217	238	±9.4
C4	241	248	245	247	252	±4.0
C5	252	260	246	260	275	±10.8
C6	276	274	272	250	246	±14.3
C7	242	248	245	232	241	±6.0
b.						
Composite	**Sample 1**	**Sample 2**	**Sample 3**	**Sample 4**	**Sample 5**	**Std. Deviation**
C1	129	131	126	127	132	±2.5
C2	92	96	92	87	94	±3.3
C3	72	74	78	76	71	±2.8
C4	86	82	88	86	89	±2.6
C5	94	92	91	88	96	±3.0
C6	94	96	94	100	97	±2.4
C7	94	86	97	92	89	±4.2
c.						
Composite	**Sample 1**	**Sample 2**	**Sample 3**	**Sample 4**	**Sample 5**	**Std. Deviation**
C1	21.44	21.48	21.52	21.54	21.52	±0.04
C2	21.24	21.12	21.16	21.1	21.28	±0.08
C3	21.04	20.92	20.88	21.04	20.92	±0.07
C4	21.12	21.08	21.16	20.98	20.96	±0.09

Table 5. *Cont.*

c.						
Composite	**Sample 1**	**Sample 2**	**Sample 3**	**Sample 4**	**Sample 5**	**Std. Deviation**
C5	21.08	21.04	21.2	21.06	21.12	±0.06
C6	21.12	21.12	21.16	21.3	21.2	±0.07
C7	21.04	20.96	20.96	21.06	21.08	±0.06

The incorporation of carbon fabric at 10 wt.% yields optimal mechanical performance, surpassing compositions of C2, C3, C4, C5, and C6 wt.%. The C6 composite, exhibiting superior mechanical properties, was selected as the base composite. Cenosphere filler was then added to this base composite in varying concentrations, ranging from 2.5 to 12.5 wt%. The mechanical properties of different weight percentages of cenosphere-filled C6 composites are presented in Figure 6. The test results of each sample are presented in Table 6. The results indicate that the incorporation of cenospheres significantly enhances tensile strength (σ) and Young's modulus (E), while reducing elongation at break, compared to unfilled composites. A notable increase in tensile strength (14%) and tensile modulus (18%) is observed with the addition of cenospheres from 2.5 wt.% to 10 wt.%. This improvement is attributed to the enhanced interfacial adhesion between the matrix and reinforcement, reduced inter-particle distance, and occupation of voids within the composite. The tensile modulus of the composite remains relatively unaffected with the addition of 2.5 wt.% cenospheres (87.65 GPa). However, further increases in cenosphere content led to an approximate 18% increase in tensile modulus. This finding is consistent with previous investigations [21,22], which suggest that the development of the fibrous structure is significantly influenced by the amount of cenospheres added. The addition of 10 wt.% cenospheres to the C6 composite results in a substantial 30% enhancement in tensile modulus, increasing from 87.65 GPa to 113.85 GPa. The addition of cenospheres facilitates uniform dispersion within the matrix, hindering failure propagation along the loading direction. Consequently, this leads to improved tensile strength and reduced elongation. The decreased ductility is attributed to the filler disrupting matrix mobility and deformability. The percentage elongation reduction exhibits minor variability, primarily due to increased cenosphere loading, which occupies interstitial volume and leads to an inadequate matrix, resulting in minimized percentage elongation. Notably, the 10 wt.% cenosphere-filled C6 composite exhibits maximum hardness compared to other composites. Incorporating cenospheres into carbon–glass-reinforced polyester composites significantly improves impact strength. Specifically, a 19% increase in impact strength is observed, rising from 80 kJ/m^2 to 99 kJ/m^2. This enhancement is attributed to the addition of 50 wt.% glass fabric and the incremental increase in cenosphere concentration from 2.5 wt.% to 10 wt.% A comparison with related works reveals that the incorporation of cenospheres can lead to significant enhancements in mechanical properties. For instance, studies have reported improvements in tensile strength (up to 25%), flexural strength (up to 30%), and impact resistance (up to 40%) with the incorporation of cenospheres in polymer composites. However, a further increase in cenosphere content to 12.5 wt.% leads to a decline in impact strength. This observation aligns with the findings of Alam et al. [23], who reported similar trends in the mechanical properties of glass fiber-reinforced polyester composites upon incorporation of various glass fibers and solid particles. The decline in mechanical properties beyond 10 wt.% carbon fabric content can be attributed to high carbon fabric content, leading to intensified fiber–fiber interaction, causing fibers to bundle together. This reduces the effective fiber-matrix interfacial area, resulting in decreased mechanical properties. Beyond 10 wt.% carbon fabric content, the matrix's role in load

transfer and absorption is compromised. The increased fiber content reduces the matrix's ability to distribute loads evenly, leading to decreased mechanical performance. Higher carbon fabric content can introduce porosity and defects within the composite. These defects can act as stress concentrators, reducing the composite's mechanical properties. Increased carbon fabric content can make manufacturing more challenging, leading to a higher likelihood of defects and reduced mechanical properties. The decline in mechanical properties beyond 10 wt.% carbon fabric content can be attributed to several factors. At higher weight fractions, the carbon fibers may start to aggregate, leading to a non-uniform distribution of fibers within the matrix. This results in a decrease in the overall mechanical properties of the composite. As the carbon fiber content increases, the interface between the fibers and the matrix may become more prone to defects, such as voids or cracks [24]. These defects act as stress concentrators, leading to a decrease in the mechanical properties of the composite. Furthermore, the addition of high amounts of carbon fibers may also lead to a reduction in the properties of the matrix material, such as its tensile strength or toughness [25]. Inadequate fiber-matrix bonding can also contribute to the decline in mechanical properties. Insufficient bonding between fibers and the matrix can lead to reduced load transfer efficiency, resulting in decreased mechanical properties. Additionally, high carbon fiber content can introduce residual stresses during manufacturing, which can negatively impact mechanical properties [26,27].

Table 6. a. Ultimate tensile strength results (MPa). b. Tensile modulus results (GPa). c. Hardness (Shore D).

a.						
Composite	**Sample 1**	**Sample 2**	**Sample 3**	**Sample 4**	**Sample 5**	**Std. Deviation**
C6-CN-2.5	296	303	308	312	298	±6.7
C6-CN-5	322	320	316	318	315	±2.8
C6-N-7.5	342	338	336	334	344	±4.1
C6-CN-10	362	358	346	342	352	±8.2
C6-CN-12.5	332	330	334	328	334	±2.6
b.						
Composite	**Sample 1**	**Sample 2**	**Sample 3**	**Sample 4**	**Sample 5**	**Std. Deviation**
C6-CN-2.5	94	88	86	82	87	±4.3
C6-CN-5	106	102	94	90	96	±6.3
C6-N-7.5	110	96	101	92	108	±7.6
C6-CN-10	96	120	113	115	124	±10.7
C6-CN-12.5	118	106	98	102	104	±7.5
c.						
Composite	**Sample 1**	**Sample 2**	**Sample 3**	**Sample 4**	**Sample 5**	**Std. Deviation**
C6-CN-2.5	21.16	20.96	20.88	20.92	21.08	±0.15
C6-CN-5	21.2	21.16	21.12	21.04	21.08	±0.06
C6-N-7.5	21.32	21.24	21.16	21.08	21.12	±0.1
C6-CN-10	21.32	21.44	21.24	21.2	21.12	±0.12

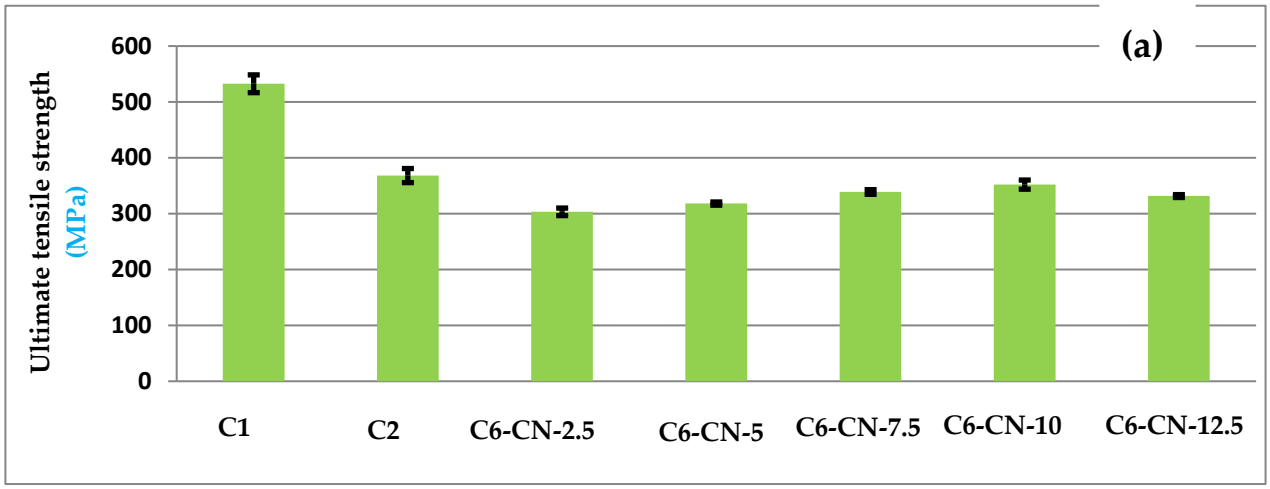

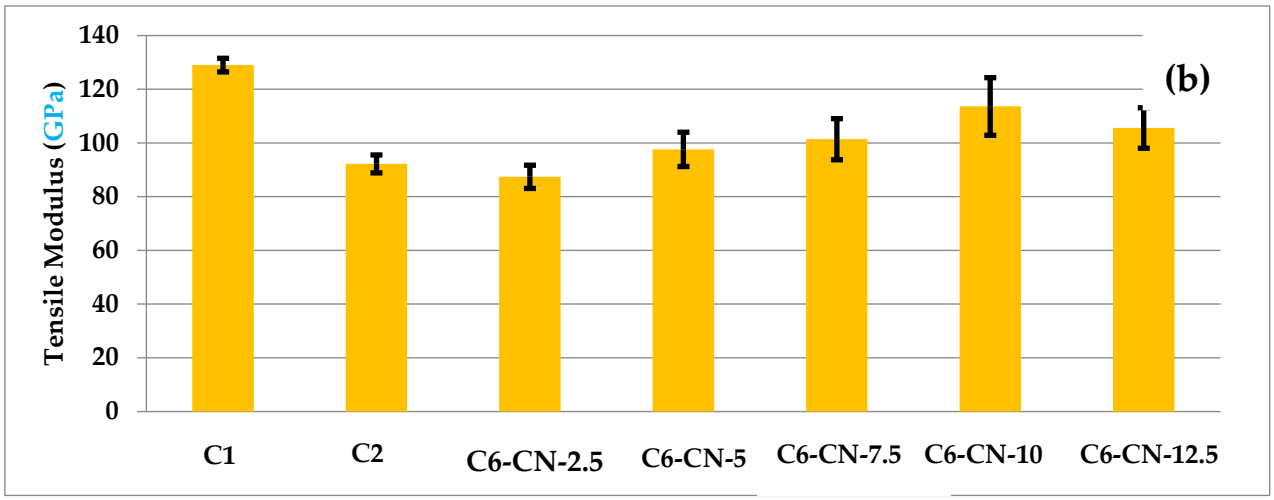

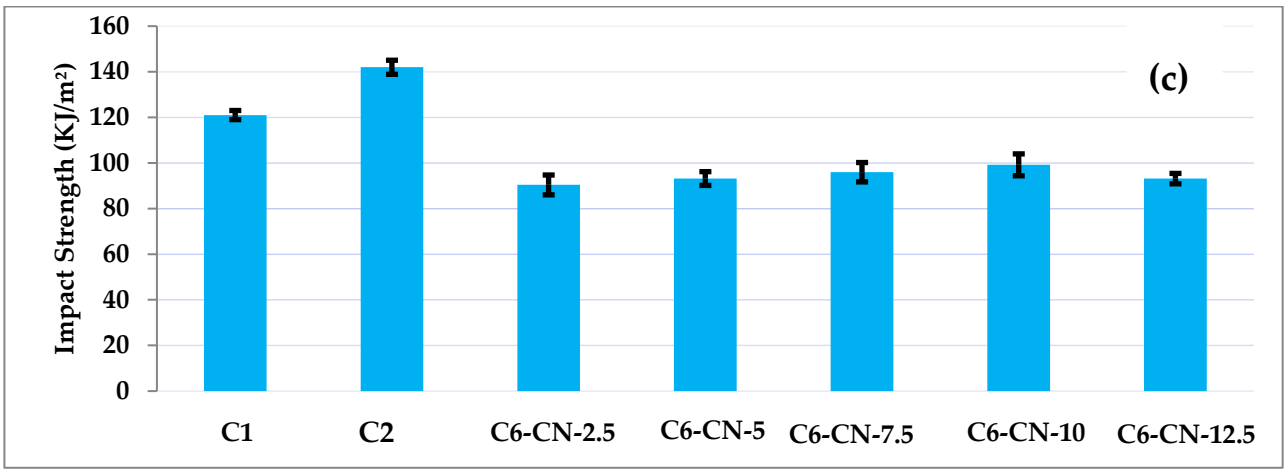

Figure 6. *Cont.*

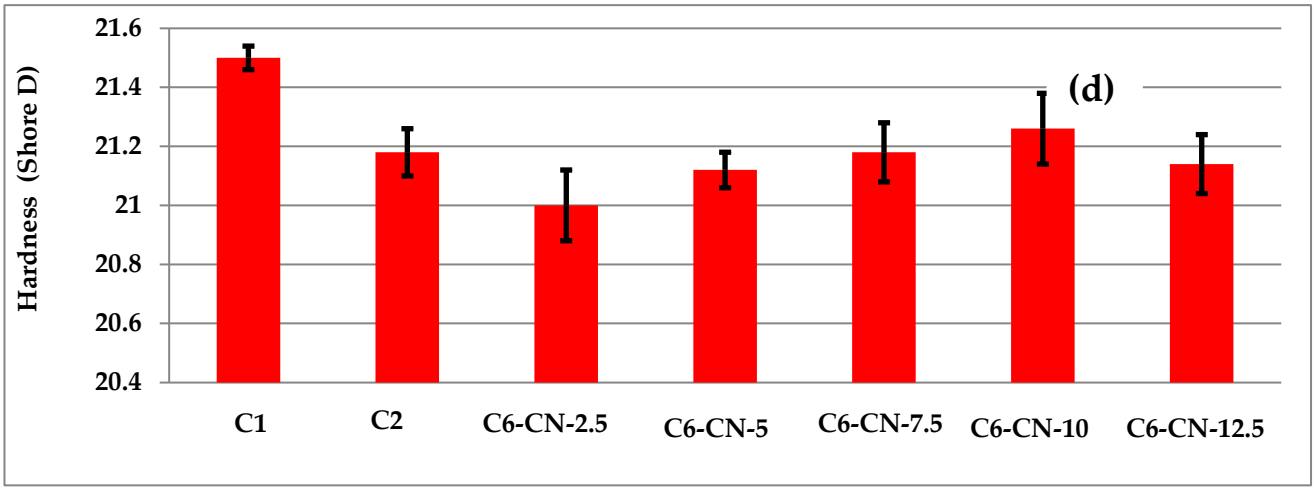

Figure 6. Mechanical properties of C1,C2, and CN filled C6 composite. (**a**) Tensile strength, (**b**) tensile modulus, (**c**) impact strength and (**d**) shore D hardness; CN: Cenosphere.

The Shore D hardness values of all composites, a combination of those with and without filler material, are presented in Figures 5d and 6d. The hardness of a carbon–glass fabric-reinforced polyester composite increased with the loading of cenosphere filler. The inclusion of cenosphere filler leads to a moderate increase in the hardness of the carbon–glass fabric-reinforced polyester composite. This can be attributed to the enhanced hardness of the composite and more uniform distribution of the cenosphere filler. The C6-CN-10 composite indicates greater hardness compared to the other composites. Lu and Komvopoulos [28] reported the indentation hardness of ultrathin amorphous carbon films. The films displayed a thickness that ranged from 7 to 95 nm and hardness values between 9 and 44 GPa. The incorporation of cenospheres into carbon–glass-reinforced polyester composites enhances surface hardness, rendering them more resistant to scratches and premature failure. Under indentation loading, the micro-particles exhibit elastic deformation, outperforming unfilled composites. The improved hardness can be attributed to the efficient load transfer facilitated by the interface between the thermoset matrix, solid fibers, and filler particles. When subjected to compressive forces, these components compress together, providing enhanced resistance and hardness.

3.2. Abrasive Wear Behavior

Figures 7 and 8 depict the variation in wear rate of the composites with increasing abrading distance and loads of 12 N and 24 N, respectively, with silica as the abrasive medium. It is observed that, as the sliding distance increases, the wear loss also increases. This is expected, as longer sliding distances typically result in more material removal. The relationship between wear loss and abrading distance appears to be non-linear, with the wear loss increasing more rapidly at higher sliding distances. The wear loss observed was considerable for carbon–glass fabric-reinforced polyester composites. The wear loss of carbon–glass fabric-reinforced composites resulting from abrasive wear escalates as the abrading distance increases. An increase loss of wear volume for C7 composite at 12.5 wt.% was observed (Figure 7a) between 2.2×10^2 mm^3 and 5×10^2 mm^3 at load of 12 N, while under a load of 24 N (Figure 8a), the wear loss varied from 2×10^2 mm^3 to 4.8×10^2 mm^3. As the load increased from 12 N to 24 N, the wear volume decreased. For the cenosphere-filled carbon–glass fabric-reinforced polyester composite (Figure 7b), it has been found that at 12.5 wt.%, the wear volume rate increases from 1.5×10^2 mm^3 to 3.8×10^2 mm^3 with a load of 12 N, while at a load of 24 N, the wear volume increases from 1.2×10^3 mm^3 to 3.6×10^3 mm^3 (Figure 8b).

In a comparison with carbon–glass fabric-reinforced composites, the cenosphere-filled carbon–glass fabric-reinforced polyester composite indicated a decreased wear volume rate at 12.5 wt.%.

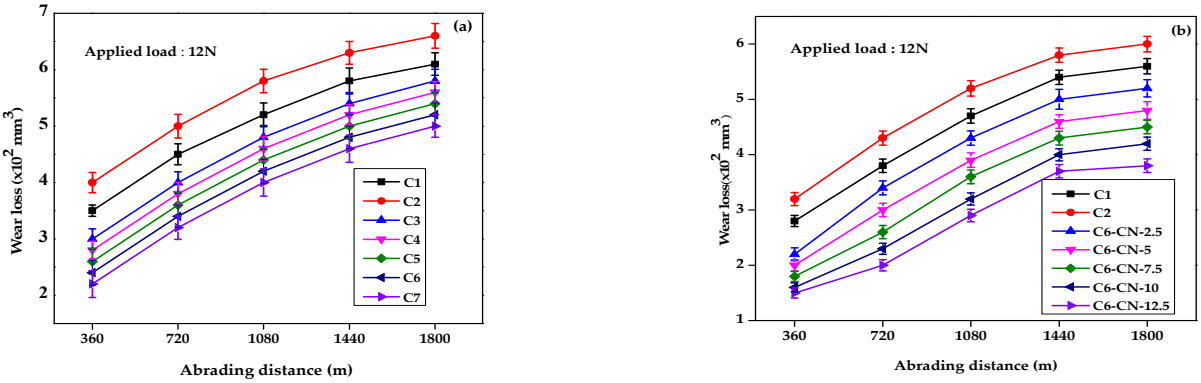

Figure 7. Wear volume of composites load-12 N (**a**) carbon–glass fabric-reinforced composites and (**b**) C1,C2, and cenosphere filled C6 composites.

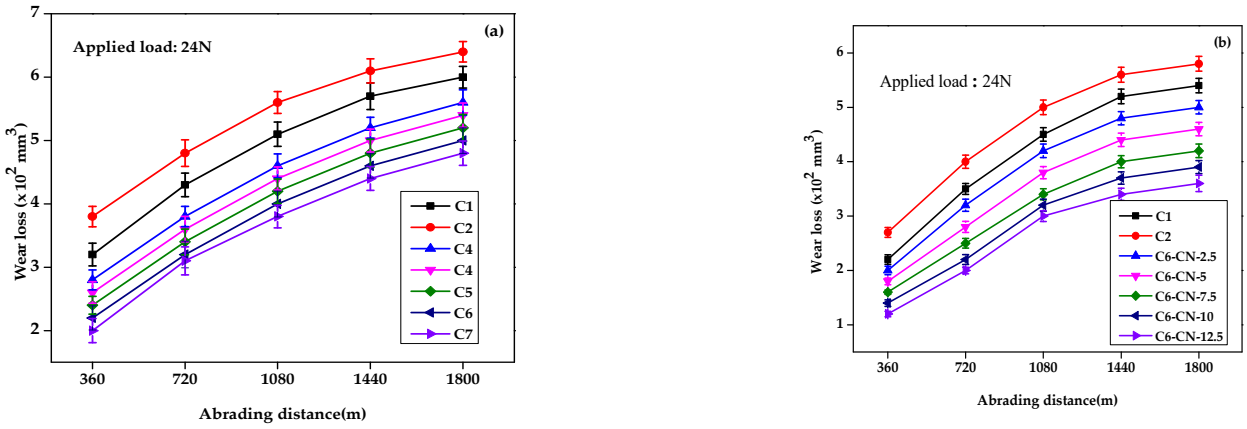

Figure 8. Wear volume of composites at load-24 N (**a**) carbon–glass fabric-reinforced composites and (**b**) C1,C2, and cenosphere filled C6 composites.

When the hard abrasive particles become entangled between the composite sample and the stainless-steel wheel, a plowing action develops on the surface. This plowing action eliminates more matrix material due to the elevated tension of the abrasive particles. Less wear loss has been found in composites C6-CN-12.5. The high cenosphere concentrations on the surface of the C6-CN-12.5 composite creates an effective barrier, limiting substantial deformation of the polyester matrix. Enhanced cenosphere loading in C6 composites has been proposed, resulting in a harder surface, therefore, contributing to the reduced wear loss reported with these composites. The wear resistance of the different composites in this study exhibited the following order for cenosphere-filled carbon–glass fabric-reinforced polyester composite: C6-CN-12.5 > C6-CN-10 > C6-CN-10 > C6-CN-2.5 > C1 > C2. The increasing wear loss with sliding distance suggests abrasive wear as a dominant mechanism and the non-linear relationship between wear loss and sliding distance may indicate adhesive wear contributions.

3.3. Specific Wear Rate (Ks)

Figures 9 and 10 show the variation in specific wear rate of different composite systems against silica abrasive, plotted as a function of abrading distance under constant loads of 12 N and 24 N, respectively. The specific wear rate decreases as the abrading distance increases. This suggests that the composite material becomes more wear-resistant as it is subjected to longer abrading distances. The specific wear rate decreases

rapidly at lower abrading distances (360–720), indicating a significant improvement in wear resistance during the initial stages of abrading. At higher abrading distances (1080–1800), the specific wear rate continues to decrease, but at a more gradual rate. The C7 composite depicts low specific wear rate compared to the entire abrading distance and applied load of 12 N and 24 N. Notably, C6-CN-12.5 composite exhibits the lowest wear rate across all sliding distances. In three-body abrasion, the wear rate is significantly influenced by the hardness of the counterbody. Abrasive particles may become embedded in the softer surface, causing it to groove the harder surface. This results in substantial damage to the fiber and polyester matrix when using silica sand abrasive, leading to an increased specific wear rate. The rapid decrease in specific wear rate at lower abrading distances suggests a running-in wear mechanism, where the composite material undergoes an initial period of high wear rate followed by a decrease in wear rate as the surface becomes smoother. The gradual decrease in specific wear rate at higher abrading distances indicates a steady-state wear mechanism, where the wear rate becomes relatively constant as the composite material reaches a stable wear condition.

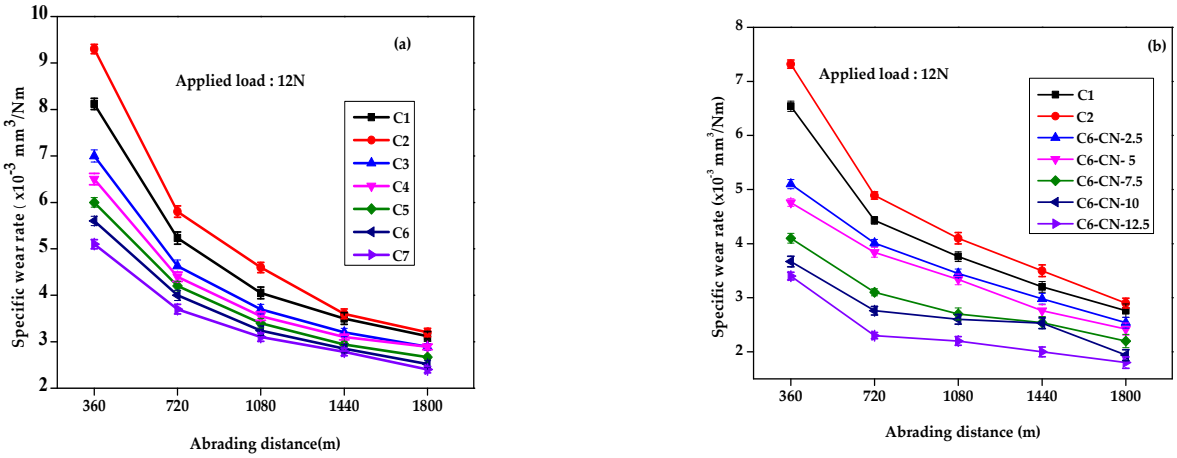

Figure 9. Specific wear rate of composites at load-12 N (**a**) carbon–glass fabric-reinforced and (**b**) cenosphere C6 composites.

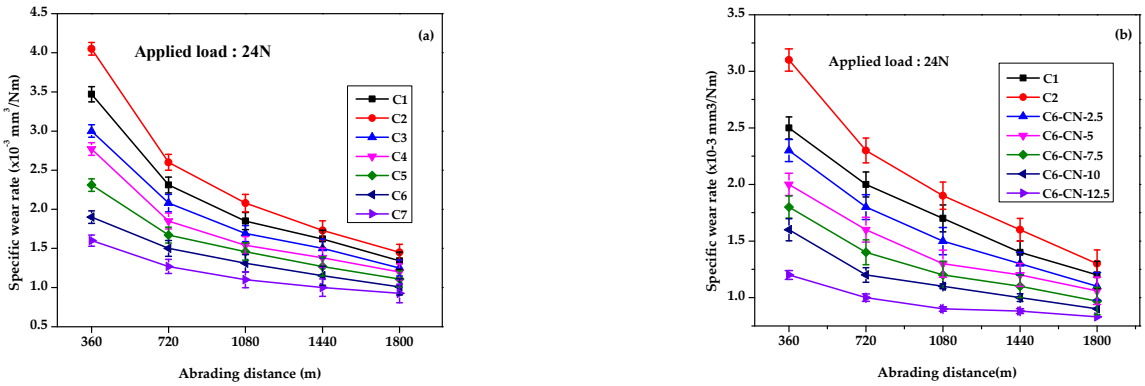

Figure 10. Specific wear rate of composites at load-24 N (**a**) carbon–glass fabric-reinforced and (**b**) cenosphere filled C6 composites.

The degradation of the unfilled carbon–glass-reinforced polyester composite is attributed to the softening of the polyester matrix under increased contact pressure. This softening leads to an increase in debris and micro-cracks within the matrix, ultimately resulting in severe fiber loss. The polymer matrix fails to protect the carbon fibers from separation, compromising the composite's wear resistance. In contrast, the incorporation of

cenospheres into the carbon–glass fabric-reinforced polyester composite enhances material toughness. The cenospheres propagate across the pockets of the carbon–glass fabrics, allowing embedded particles to roll easily instead of splitting the fibers. This mechanism improves the composite's wear resistance and overall performance.

3.4. Interdependence Between Wear and Mechanical Properties

Extensive research has explored the relationship between wear loss and mechanical properties, including the e-factor and hardness, in single-pass abrasive wear tests of unfilled polymers and composites. Lancaster [29] highlighted the significant impact of the product of tensile strength and ultimate elongation on the abrasive wear behavior of composites. The addition of fiber or filler reinforcement typically enhances the tensile strength of the neat polymer but may compromise its elongation at break, resulting in a lower e-factor. Consequently, reinforcement often leads to reduced abrasive wear resistance. A proposed model reveals an inverse relationship between material removal rate and the product of stress and strain at rupture. The wear volume loss is found to decrease with increasing e-factor, consistent with previous reports [30,31]. Specifically, the 10 wt.% cenosphere-filled sample exhibits the lowest wear volume loss, and its corresponding value normalized by the e-factor product is also the lowest, in agreement with published literature [32].

3.5. Worn out Morphology Analysis

Figures 11 and 12 present the SEM worn surfaces for the C6 composite and the C composite samples for constant abrading sliding distance of 1800 m and load of 12 N and 24 N, respectively. The SEM images show significant wear on the surface. The polyester matrix, in addition to carbon and glass fibers, indicates more damage in unfilled carbon–glass polyester composites when compared with cenosphere-filled carbon–glass polyester composite samples. Severe damage to the fiber causes greater fiber loss from the worn surface. The C6 composite (Figure 11) exhibits severe damage, including fiber pullout, disorientation, and extensive matrix damage, with embedded silica sand particles. In contrast, the C6-CN-10 composite (Figure 12) displays a relatively smooth worn surface, characterized by micro-cracks within the matrix, minimal fiber damage, limited silica particle embedment, and strong interfacial adhesion between fiber, filler, and matrix.

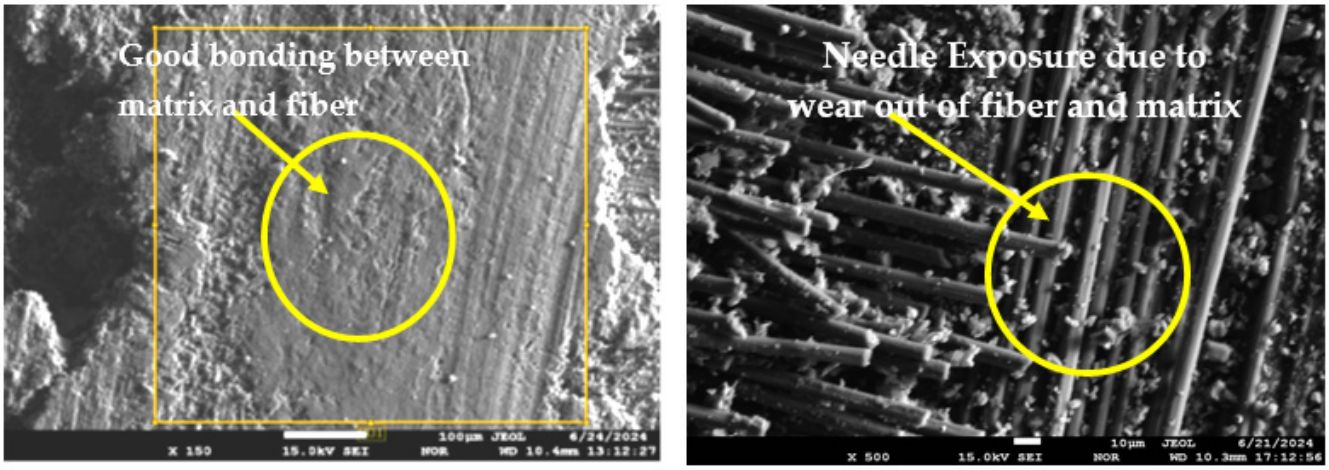

Figure 11. SEM worn morphology of C6 composite at load (**a**) 12 N and (**b**) 24 N.

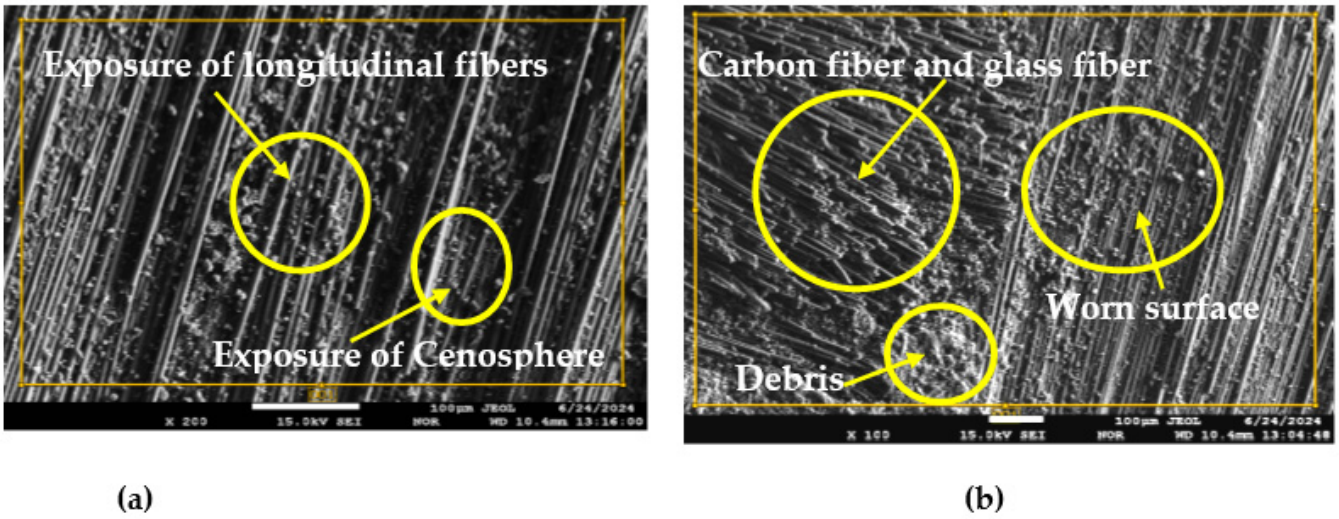

Figure 12. SEM worn morphology of C6-CN-10 composite samples at load (**a**) 12 N and (**b**) 24 N.

These observations indicate that the addition of cenospheres enhances the abrasion resistance of the composite. It observed that the smooth worn surface of cenosphere-filled carbon–glass polyester composite exhibits a smooth feature compared to unfilled carbon–glass polyester composite samples under 12 and 24 N load applications. The observed features indicate that wear loss is greater in C6 composite samples than in those C6-CN-10 composite samples. In the C6-CN-10 composite sample, less broken fibers and minimal debris formation are evident. In contrast, the unfilled carbon–glass polyester composite sample exhibits fiber debonding accompanied by cleavage-type fractures. The SEM analysis of the C6 composite sample reveals a large number of broken fibers, considerable deformation in the matrix, and an increased debris formation. The study demonstrates that the incorporation of cenosphere filler, particularly at theC6-CN-10 composite, significantly enhances the abrasive wear resistance and mechanical behavior of carbon–glass polyester composites. This finding confirms that cenosphere filler reinforcement improves both the mechanical and tribological properties of composites.

4. Conclusions

This study investigates the abrasive wear performance of cenosphere-filled glass–carbon fabric reinforced polyester composites, examining the effects of cenosphere content, abrasive distance, and applied load. Key inferences from the findings are as follows:

- The addition of cenospheres reduces wear volume and specific wear rate in the composites. The current investigation has yielded the following outcomes:
- Fully dense composites encompassing bidirectional carbon–glass fabric-reinforced polyester and cenosphere-filled carbon–glass fabric-reinforced polyester were successfully fabricated. Cenosphere-filled carbon–glass fabric-reinforced polyester composites proved to have better tensile strength and modulus, in addition to decreased elongation at break, when compared with unfilled carbon–glass fabric-reinforced polyester composites;
- The composite containing 10 wt.% cenospheres (C6-CN-10) composite demonstrated enhanced tensile strength and modulus, accompanied by a relatively minimal reduction in elongation at break compared to unfilled and lower-filled composites;
- The inclusion of silica as an abrasive material considerably lowered the specific wear rate of the composites.

- ➢ Cenospheres proved to be effective fillers, enhancing both abrasion resistance and mechanical properties. These improvements make the composites well-suited for applications involving abrasive wear.
- ➢ Cenospheres act as effective filler materials, improving the abrasion resistance and mechanical properties of carbon–glass fabric-reinforced polyester composite samples. Therefore, adding more cenosphere to carbon–glass fabric-reinforced polyester composites is advantageous for applications that involve abrasive wear conditions.

Author Contributions: K.H.P.: literature search, methodology, conducted experimental tests on composites, and performed data processing/analysis and drafting; D.M.G.: conceptualization, data curation, review, editing, and supervision; R.V.K.: review, editing, and supervision. D.G.P.: contributed to result interpretation and the discussion of the selected results. All authors helped with the collection of data from the scientific literature review, organized the results obtained from the scientific community, and wrote the manuscript writing. All authors have read and agreed to the published version of the manuscript.

Funding: This research received no external funding.

Data Availability Statement: The data presented in this study are available within the article.

Acknowledgments: The authors would like to thank the support granted by the GeoBioTec Research Unit, through the projects UIDB/04035/2020 (https://doi.org/10.54499/UIDB/04035/2020) and UIDP/04035/2020 (https://doi.org/10.54499/UIDP/04035/2020), funded by the Foundation for Science and Technology, IP/MCTES through national funds (PIDDAC).

Conflicts of Interest: The authors declare no conflicts of interest.

References

1. Schwartz, M.M. *Composite Materials Handbook*; McGraw-Hill: New York, NY, USA, 1992.
2. Maiti, S.N.; Lopez, B.H. Tensile properties of polypropylene/kaolin composites. *J. Appl. Polym. Sci.* **1992**, *44*, 353–360. [CrossRef]
3. Hutchings, I.M. *Tribology: Friction and Wear of Engineering Materials*; CRC Press: London, UK, 1992; pp. 156–164.
4. El-Tayeb, N.S.M.; Yousif, B.F.; Yap, T.C. Tribological studies of polyester reinforced with CSM 450 R glass fiber sliding against smooth stainless steel counter face. *Wear* **2006**, *261*, 443–452. [CrossRef]
5. El-Tayeb, N.S.M.; Yousif, B.F. Evaluation of glass fibre reinforced polymer composites for multi-pass abrasive wear applications. *Wear* **2007**, *262*, 1140–1151. [CrossRef]
6. Pihitili, H.; Tosun, N. Effect of load and speed on the wear behaviour of woven glass fabrics and armid fibre reinforced composites. *Wear* **2002**, *252*, 979–984. [CrossRef]
7. Bhawani, S.T.; Michael, J.F. Tribological behavior of uni-directional graphite epoxy and carbon-PEEK composite. *Wear* **1993**, *162*, 385–396.
8. Mody, P.B.; Chou, T.W.; Friedrich, K. Effect of testing conditions and microstructure on the sliding wear of graphite fiber/PEEK matrix composites. *J. Mater. Sci.* **1988**, *23*, 4319–4330. [CrossRef]
9. Tsukizoe, T.; Ohmae, N. Wear mechanism of unidirectionally oriented fiber reinforced plastics. *J. Lubr. Technol.* **1977**, *99*, 401–407. [CrossRef]
10. Suresha, B.; Chandramohan, G.; Siddaramaiah; Shivakumar, K.N.; Ismail, M. Mechanical and three-body abrasive wear behaviour of three dimensional glass-fabric reinforced vinyl ester composite. *Mater. Sci. Eng. A* **2008**, *480*, 573–579. [CrossRef]
11. Suresha, B.; Chandramohan, G. Three-body abrasive wear behaviour of particulate filled glass–vinyl ester composites. *J. Mater. Process Technol.* **2008**, *200*, 306–311. [CrossRef]
12. Devi, M.S.; Murugesan, V.; Rengaraj, K.; Anand, P. Utilization of fly ash as filler for unsaturated polyester resin. *J. Appl. Polym. Sci.* **1998**, *69*, 1385–1391. [CrossRef]
13. Maher, M.H.; Balaguru, P.N. Properties of flowable high-volume fly ash-cement composite. *J. Mater. Civ. Eng.* **1993**, *5*, 212–225. [CrossRef]
14. Biswas, S.; Satpathy, A. Tribo-performance analysis of red mud filled glass epoxy composites using Taguchi experimental design. *Mater. Des.* **2009**, *30*, 2841–2853. [CrossRef]
15. Suresha, B.; Chandramohan, G.; Siddaramaiah; Jayaraju, T. Influence of cenosphere filler additions on three body abrasive wear behavior of glass fiber-reinforced epoxy composites. *Polym. Sci.* **2008**, *29*, 307–312. [CrossRef]

16. Cirino, M.; Friedrich, K.; Pipes, R.B. The abrasive wear behavior of continuous fiber polymer composites. *J. Mater. Sci.* **1987**, *22*, 2481–2492. [CrossRef]
17. Cirino, M.; Friedrich, K.; Pipes, R.B. Evaluation of polymer composites for sliding and abrasive wear applications. *Composites* **1988**, *19*, 383–392. [CrossRef]
18. Cenna, A.; Doyle, J.; Page, N.; Beehag, A.; Dastoor, P. Wear mechanisms in polymer matrix composite abraded by bulk solids. *Wear* **2000**, *240*, 207–214. [CrossRef]
19. Hao, W.; Liu, Y.; Neagu, A.; Bacsik, Z.; Tai, C.W.; Shen, Z.; Hedin, N. Core-shell and hollow particles of carbon and sic prepared from hydrochar. *Materials* **2019**, *12*, 1835. [CrossRef]
20. Singh, S. Chemical Composition of Cenosphere. *Materials* **2020**, *13*, 234.
21. Chand, N.; Naik, A.M.; Neogi, S. Three-body abrasive wear of short glass fiber polyester composite. *Wear* **2000**, *242*, 38–46. [CrossRef]
22. Satapathy, A.; Patnaik, A.; Biswas, S. Investigations on three-body abrasive wear and mechanical properties of particulate filled glass epoxy composites. *Malaysian Polym. J.* **2010**, *5*, 37–48.
23. Alam, S.; Habib, F.; Irfan, M. Effect of orientation of glass fiber on mechanical properties of GRP composites. *J. Chem. Soc. Pak.* **2010**, *32*, 265–269.
24. Liu, J.; He, L.; Yang, D.; Liang, J.; Zhao, R.; Wang, Z.; Li, X.; Chen, Z. Effects of Carbon Fiber Content on the Crystallization and Rheological Properties of Carbon Fiber-Reinforced Polyamide 6. *Polymers* **2024**, *16*, 2395. [CrossRef]
25. Khakalo, S.; Niiranen, J. Lattice structures as thermoelastic strain gradient metamaterials: Evidence from full-field simulations and applications to functionally step-wise-graded beams. *Compos. Part B Eng.* **2019**, *177*, 107224. [CrossRef]
26. Fan, K.; Zhang, M.; Shang, C.; Saba, F.; Yu, J. Mechanical properties of carbon fiber-reinforced polymer composites: A review. *Compos. Part A Appl. Sci. Manuf.* **2020**, *130*, 105834. [CrossRef]
27. Berton, T.; Najafi, F.; Singh, C.V. Development and implementation of a multi-scale model for matrix micro-cracking prediction in composite structures subjected to low velocity impact. *Compos. Part B Eng.* **2019**, *168*, 140–151. [CrossRef]
28. Lu, W.; Komvopoulos, K. Nano tribological and nano mechanical properties of ultrathin amorphous carbon films synthesized by radio frequency sputtering. *J. Tribol.* **2001**, *123*, 641–650. [CrossRef]
29. Lancaster, J.K. Friction and wear. In *Polymer Science: A Material Science Hand Book*; Jenkins, A.D., Ed.; Elsevier: Amsterdam, The Netherlands, 1972; pp. 959–1046.
30. Zhang, H.S.; Komvopoulos, K. Direct-current cathodic vacuum arc system with magneticfield mechanism for plasma stabilization. *Rev. Sci. Instrum.* **2008**, *79*, 073905. [CrossRef]
31. Suresha, B.; Chandramohan, G.; Kishore; Sampathkumaran, P.; Seetharamu, S. Mechanical and three-body abrasive wear behaviour of SiC filled glass-epoxy composites. *Polym. Compos.* **2008**, *29*, 1020–1025. [CrossRef]
32. Ratner, S.B.; Farberova, I.I.; Radyukevich, O.V.; Lure, E.G. Correlations between wear resistance and other mechanical properties. *Sov. Plast.* **1964**, *7*, 37–45.